Temporally Staggered Sensors in Multi-Sensor Target Tracking Systems

RUIXIN NIU
PRAMOD K. VARSHNEY, Fellow, IEEE
KISHAN MEHROTRA
CHILUKURI MOHAN
Syracuse University

For a multi-sensor target tracking system, the effects of temporally staggered sensors on system performance are investigated and compared with those of synchronous sensors. To capture system performance over time, a new metric, the average estimation error variance (AEV), is proposed.

For a system that has N sensors with equal measurement noise variance, numerical results show that the optimal staggering pattern is to use N uniformly staggered sensors. We have also shown analytically that the AEV of the system with N uniformly staggered sensors is always smaller than that of the system with N synchronous sensors.

For sensors with different measurement noise variances, the optimal staggering pattern can be found numerically. Practical guidelines on selecting the optimal staggering pattern have been presented for different target tracking scenarios. Due to its simplicity, uniform staggering can be used as an alternative scheme with relatively small performance degradation.

Manuscript received August 15, 2002; revised May 18 and November 30, 2004; released for publication January 12, 2005.

IEEE Log No. T-AES/41/3/856422.

Refereeing of this contribution was handled by D. J. Salmond and T. Kirubarajan.

This work was supported by the DoD Multidisciplinary University Research Initiative (MURI) program administered by the Army Research Office under Grant DAAD19-00-1-0352.

Part of this work was presented at the Fusion '02 Conference.

Authors' address: Dept. of Electrical Engineering and Computer Systems, Syracuse University, 335 Link Hall, Syracuse, NY 13244, E-mail: (varshney@ecs.syr.edu).

I. INTRODUCTION

Almost all conventional target tracking systems, both single sensor and multi-sensor, rely on sensors that provide measurements on a regular schedule, i.e., on a fixed-interval basis. This is due to technical limitations of sensors such as sonar and rotating radars, and also due to the desire to keep operational systems as simple as possible. Electronically scanned radars allow the possibility of altering the regular schedule by collecting measurements in a nonuniform manner. Recently, Daum [6] and Zhang, et al. [16] have suggested that this additional degree of freedom for nonuniformly scheduled measurements be exploited to enhance system performance. In fact, this issue of temporal effects has been studied by Zhang et al. [16] in some detail. They have compared the performance of nonuniform sampling schemes with that of uniform sampling schemes. They found that if a multi-scan tracker is used, then nonuniform sampling could outperform uniform sampling. This is a significant result in that it establishes the importance of measurement scheduling in tracking.

There has been an increasing interest in employing multiple sensors for target tracking due to the significantly improved estimation accuracy and robustness of the system. In [2] and [12], different types of multi-sensor tracking system architectures are discussed and algorithms for tracking and fusion are presented. In almost all the system architectures considered, measurements are assumed to arrive synchronously and temporal effects of the measurement process are ignored. In practice, maintenance of synchronism is difficult and measurements arrive in an asynchronous manner that are often out of sequence. Recently, many authors have investigated the so-called problem of "out of sequence measurements (OOSM)." This means in a multi-sensor system, a delayed measurement with time stamp τ arrives after the target state has been updated to time $t > \tau$. In [3] an exact solution to update with OOSMs for the single lag case is presented for the linear dynamic and linear measurement models with additive Gaussian noises. An algorithm to deal with multiple lags and multiple dynamic models is developed in [10]. In [4] authors use a one-step solution to solve the general OOSM problem with multiple lags. An exact solution to update with OOSMs for the multiple-lag case for the linear dynamic and linear measurement models with additive Gaussian noises is presented in [15]. In [11] authors present a multiple-lag OOSM algorithm for a dwell-based multi-sensor multi-target multi-hypothesis tracking system with missed detections and clutter.

While the OOSM problem has recently been considered, not much attention has been paid to multi-sensor tracking systems with asynchronous sensors, which collect observations at different

times. The lack of synchronization can be just the result of a real-life system with sensors that have coarse synchronization, and/or the result of a system with sensors with different sampling rates. Another possibility is that the sensors are deliberately designed to be temporally staggered for potential performance enhancement. This sensor time management function could be implemented as a part of level 4 fusion of the JDL fusion process model [9]. We explore here the issue of temporally staggered sensing in multi-sensor tracking systems in some detail. This idea was independently mentioned in a related work [16]. Our work is different from [16]. In [16], authors compared the uniform and nonuniform sampling schemes for single-sensor systems. There, numerical and simulation results were given to compare the performances in terms of the traditional metrics, namely the estimation error variance and track life. We investigate temporal staggering schemes for multi-sensor systems. Many analytical closed-form results are provided and the performances are compared and studied in terms of several new metrics, which are introduced to measure the estimation accuracy over time.

We also investigate the following issues related to asynchronous sensors.

1) What are the effects of asynchronous sensors on system performance?
2) Can we benefit from asynchronous sensors in terms of performance?
3) If so, how can we design the asynchronous or temporal staggering pattern to maximize the benefit?

The scheme using staggered sensors may seem very unusual at first. In a multi-sensor target tracking system, estimation accuracy with asynchronous sensors right after the system is updated with new measurements is not as good as a system with synchronous sensors. However, we see later in this work that system performance is enhanced based on the metrics that we define. Here we assume the absence of false alarms and missed detections. The presence of these is addressed in [14].

In Section II, we introduce the dynamic model of the target and the corresponding steady state estimation error covariance matrix. For simplicity, we assume there is only one target in the whole surveillance region of the tracking system. In Section III, a simple example is given that provides the motivation for the use of staggered sensors. We also define a new metric to measure the performance of the tracking system—the error variance averaged over time (AEV). In Section IV, for the case of multiple sensors with the same measurement noise variance, we numerically find the optimal staggering scheme and derive corresponding analytical results. In Section V, the case where multiple sensors have different measurement noise variances is studied, and the best pattern for staggering sensors is found numerically. The conclusions are drawn in Section VI.

II. SYSTEM MODEL

A 1-dimensional direct discrete white noise acceleration model [1] is used here. An alternative is the discretized continuous white noise acceleration model. Both of them are approximations of the target motion and there is little difference between them. We choose the direct discrete time white noise acceleration model because of the availability of the closed-form steady state error covariance matrix for this model, which makes our analysis much easier.

We assume a target moving along a coordinate ξ, and the state of the target is

$$x = [\xi \quad \dot{\xi}]'. \tag{1}$$

The state equation for the piecewise constant white acceleration model is

$$x(k+1) = Fx(k) + \Gamma \nu(k) \tag{2}$$

where

$$F = \begin{bmatrix} 1 & T \\ 0 & 1 \end{bmatrix} \tag{3}$$

$$\Gamma = \begin{bmatrix} \frac{T^2}{2} \\ T \end{bmatrix} \tag{4}$$

and T is the sampling interval of the system. The process noise covariance matrix is

$$\begin{aligned} Q &= E[\Gamma \nu(k)\nu(k)\Gamma'] \\ &= \sigma_\nu^2 \begin{bmatrix} \frac{T^4}{4} & \frac{T^3}{2} \\ \frac{T^3}{2} & T^2 \end{bmatrix}. \end{aligned} \tag{5}$$

The measurement model is

$$z(k) = Hx(k) + \omega(k). \tag{6}$$

We assume that only position (range) measurements are available, meaning that

$$H = [1 \quad 0]. \tag{7}$$

The measurement noise autocorrelation function is

$$E[\omega(k)\omega(j)] = \sigma_\omega^2 \delta_{kj}. \tag{8}$$

The target maneuvering index [1] is defined as

$$\lambda = \frac{\sigma_\nu T^2}{\sigma_\omega}. \tag{9}$$

λ, which is the ratio of the motion uncertainty and the observation uncertainty, measures the degree of elusiveness of the target to be tracked; for a fixed σ_ω, higher λ implies larger uncertainty about the motion of the target.

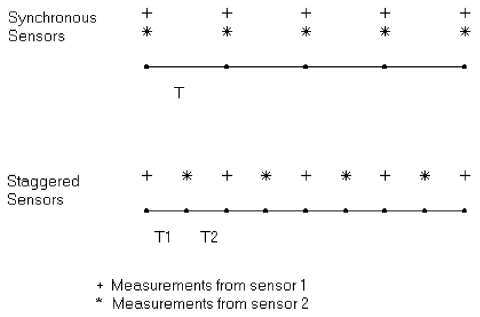

Fig. 1. Measurement pattern for two synchronous sensors versus two staggered sensors. Sampling intervals satisfy $T = T_1 + T_2$.

In [1, 7, 8], the steady state filter, known as the α-β filter, and its closed-form expression for the steady state error covariance are available when the system has a constant sampling interval.

The steady state estimation error covariance matrix is

$$P = \begin{bmatrix} p_{11} & p_{12} \\ p_{12} & p_{22} \end{bmatrix} = \sigma_\omega^2 \begin{bmatrix} \alpha & \dfrac{\beta}{T} \\ \dfrac{\beta}{T} & \dfrac{\beta(\alpha - \beta/2)}{T^2(1-\alpha)} \end{bmatrix} \tag{10}$$

where

$$\alpha = -\tfrac{1}{8}(\lambda^2 + 8\lambda - (\lambda+4)\sqrt{\lambda^2+8\lambda}) \tag{11}$$

$$\beta = \tfrac{1}{4}(\lambda^2 + 4\lambda - \lambda\sqrt{\lambda^2+8\lambda}). \tag{12}$$

The analysis is performed here in only one dimension. However, the results can be easily extended to multi-dimensional cases if the target dynamics and measurements in different dimensions are independent (uncoupled).

III. NEW PERFORMANCE METRIC

A. Motivating Example

First of all, we denote the time just before and just after the new measurements arrive at the conventional tracker with synchronous measurements as

$$kT^- \quad \text{and} \quad kT^+, \qquad k = 1,2,\ldots$$

respectively, where T is the sampling interval. Let us consider two different data collection schemes for a two-sensor tracking system, as shown in Fig. 1. In one system, both sensors collect data at the same time kT; while in the other system, one sensor collects measurements at kT, and the other one at $kT + T_1$. Both systems process data in a centralized manner.

The transient and steady state position estimation error variances based on the model introduced in Section II for these two systems are plotted in Figs. 2 and 3. In this particular case, we assume $T_1 = T_2 = T/2$

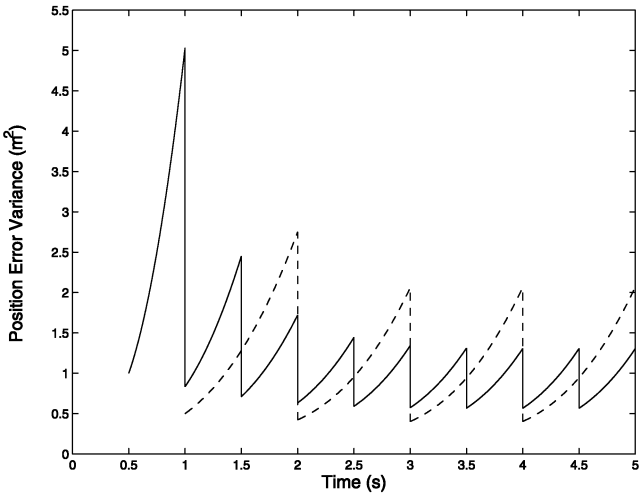

Fig. 2. Transient position estimation error variances for system with synchronous sensors (dashed line) and system with temporally staggered sensors (solid line) as illustrated in Fig. 1. $T = 1$ s, $T_1 = T_2 = 0.5$ s, SD of measurement noise at two sensors: $\sigma_{\omega_1} = \sigma_{\omega_2} = 1$ m, SD of state process noise for synchronous sensors: $\sigma_\nu = 1$ m/s^2.

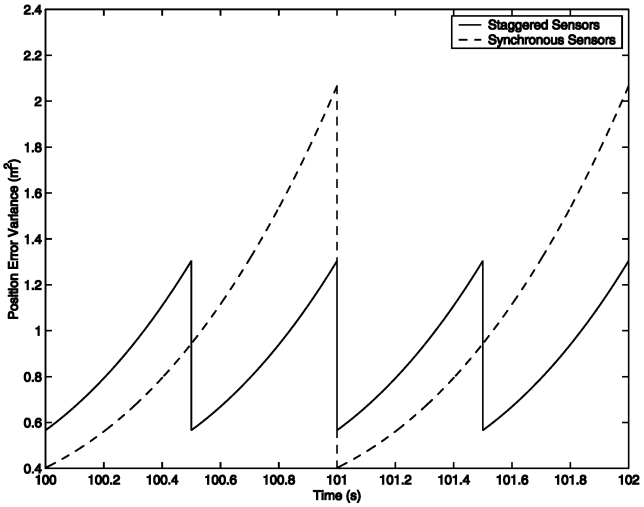

Fig. 3. Steady state position estimation error variances for system with synchronous sensors and system with temporally staggered sensors as illustrated in Fig. 1. System parameters are same as those listed in Fig. 2.

and the two sensors have the same measurement noise variance. In both systems, their Kalman filters are initialized using two-point differencing [1]. As shown in Fig. 2, the system with temporally staggered sensors always has a smaller maximum prediction error variance than the system with synchronous sensors, except its prediction made just one step after the initialization of its Kalman filter, which has the largest error variance. As we can see in Figs. 2 and 3, after the systems reach the steady state, at time kT^+, the system with synchronous sensors has a better performance than that with temporally staggered sensors. This is because at each updating time kT, it has two measurements, i.e., more information about

the target. For the system with staggered sensors, although the performance is a little worse between kT^+ and $(k+\frac{1}{2})T^-$, it has much better performance between $(k+\frac{1}{2})T^+$ and $(k+1)T^-$ due to its more frequently updated data. Also, the maximum value of the position error variance is much smaller in the staggered sensors case. This suggests that temporally staggered sensors are a better choice when the major concern of the system is to keep maximum prediction error or average estimation error low. It motivates us to explore different sensor staggering schemes over time.

For a nonlinear system with a nonlinear measurement equation (sensor nonlinearity), a well-known estimator is the first- or second-order extended Kalman filter (EKF) [1], which is obtained by a Taylor series expansion of the measurement equation around the predicted target state, with terms up to first or second order. Temporally staggered sensors give rise to a smaller steady state prediction error just before the update of the target state, as shown in the above example and later in this work. This could be of potential benefit for the EKF, because smaller prediction error means that the predicted target state is closer to the true target state, and thus the approximation by Taylor series expansion is more accurate. However, for simplicity, we concentrate on the effect of sensor staggering on linear systems in the steady state regime in this paper.

B. New Metric-Generalized Error Variance

From Section IIIA and Fig. 3, we note that as a function of time, the nature of estimation error variance for the system with synchronous sensors and the system with staggered sensors are quite different. In order to capture the system performance over time, we define a new metric which can facilitate different types of performance evaluation and comparisons. The generalized error variance (GEV) is defined as

$$\text{GEV} = \int_{kT}^{(k+1)T^-} V(t)w(t)dt \tag{13}$$

where $w(t)$ is a weighting function which satisfies

$$\int_{kT}^{(k+1)T^-} w(t)dt = 1 \tag{14}$$

and $V(t)$ is the estimation error variance. In (13) and (14), k should be large enough such that the system has reached steady state.

Actually, $w(t)$ specifies how important the system performance at a specific time is. For example, if

$$w(t) = \delta(t - kT^+) \tag{15}$$

then the metric GEV is the estimation error variance just after the system is updated with new measurements. We call it the updated estimation error variance (UEEV), and call the corresponding covariance matrix as updated covariance matrix (UCM).

For

$$w(t) = \delta(t - (k+1)T^-) \tag{16}$$

the metric GEV becomes the maximum prediction error variance (MPEV) just before the system is updated with new measurements. We call the corresponding covariance matrix as maximum covariance matrix (MCM).

If

$$w(t) = \begin{cases} \dfrac{1}{T} & kT \le t < (k+1)T \\ 0 & \text{else} \end{cases} \tag{17}$$

then GEV is the estimation error variance averaged over time. We define it as the average error variance (AEV). We call the corresponding covariance matrix as average covariance matrix (ACM). AEV is a reasonable metric because we are interested in system performance over the entire time of operation instead of at a specific time. We mainly study and compare system performance in terms of AEV.

For a Kalman filter, the steady state prediction error covariance matrix at time $kT + t$ $(0 \le t < T)$ is

$$\begin{aligned} &P(kT + t \mid kT) \\ &\quad = F(t)P(k \mid k)F(t)' + Q(t) \\ &\quad = \begin{bmatrix} 1 & t \\ 0 & 1 \end{bmatrix} \begin{bmatrix} p_{11} & p_{12} \\ p_{12} & p_{22} \end{bmatrix} \begin{bmatrix} 1 & 0 \\ t & 1 \end{bmatrix} + \frac{\sigma_\nu^2 T}{t} \begin{bmatrix} \frac{t^4}{4} & \frac{t^3}{2} \\ \frac{t^3}{2} & t^2 \end{bmatrix} \\ &\quad = \begin{bmatrix} 1 & t \\ 0 & 1 \end{bmatrix} \begin{bmatrix} p_{11} & p_{12} \\ p_{12} & p_{22} \end{bmatrix} \begin{bmatrix} 1 & 0 \\ t & 1 \end{bmatrix} + \sigma_\nu^2 T \begin{bmatrix} \frac{t^3}{4} & \frac{t^2}{2} \\ \frac{t^2}{2} & t \end{bmatrix}. \end{aligned}$$

The process noise variance σ_ν^2 in (5) is replaced here by $\sigma_\nu^2 T/t$. This is because the time at which prediction is made is a variable. To model the same amount of target motion uncertainty, the state process noise variance has to be rescaled [1].

Hence the position prediction error variance and the velocity prediction error variance at time t are

$$V_p(t) = p_{11} + 2p_{12}t + p_{22}t^2 + \tfrac{1}{4}\sigma_\nu^2 T t^3 \tag{18}$$

$$V_v(t) = p_{22} + \sigma_\nu^2 T t \tag{19}$$

resulting in the trace of the prediction error covariance matrix at time t given by

$$\begin{aligned} \text{Tr}[P(t)] &= V_p(t) + V_v(t) \\ &= p_{11} + p_{22} + (2p_{12} + \sigma_\nu^2 T)t + p_{22}t^2 + \tfrac{1}{4}\sigma_\nu^2 T t^3. \end{aligned} \tag{20}$$

IV. STAGGERING SENSORS WITH EQUAL MEASUREMENT NOISE VARIANCES

A. Optimal Staggering Schemes for Identical Sensors

We now consider the general case in which a system has N sensors and each sensor receives a position measurement corrupted by Gaussian noise with the same variance σ_ω^2. For a system with synchronous sensors operating in a centralized manner, its performance is the same as a system with one composite sensor with smaller variance σ_ω^2/N. By using (9)–(12), we can easily obtain the steady state covariance matrix P. Then the average position and velocity error variances for this system are

$$\begin{aligned}\mathrm{AEV_p} &= \frac{1}{T}\int_0^T V_p(t)dt \\ &= p_{11} + p_{12}T + \tfrac{1}{3}p_{22}T^2 + \tfrac{1}{16}\sigma_\nu^2 T^4 \end{aligned} \tag{21}$$

and

$$\begin{aligned}\mathrm{AEV_v} &= \frac{1}{T}\int_0^T V_v(t)dt \\ &= p_{22} + \tfrac{1}{2}\sigma_\nu^2 T^2 \end{aligned} \tag{22}$$

respectively.

For the system with temporally staggered sensors, each sensor has the sampling rate $1/T$ and we define the time interval between sensor S_i and the next sensor S_{i+1} as Δ_i. Therefore, we have

$$\sum_{i=1}^{N}\Delta_i = T. \tag{23}$$

Again, because the sampling intervals are variable, to model the same target motion uncertainty, the state process noise variance $\sigma_{\nu_i}^2$, which is associated with interval Δ_i, has to be rescaled. Namely

$$\sigma_{\nu_i}^2 = \frac{\sigma_\nu^2 T}{\Delta_i} \tag{24}$$

where σ_ν^2 is the state process noise variance used by the system with synchronous sensors. Then the average position error variance is

$$\begin{aligned}\mathrm{AEV_p} &= \frac{1}{T}\int_0^T V_p(t)dt \\ &= \frac{1}{T}\sum_{i=1}^{N}\left[p_{11}^i\Delta_i + p_{12}^i\Delta_i^2 + \frac{p_{22}^i\Delta_i^3}{3} + \frac{\sigma_{\nu_i}^2\Delta_i^5}{16}\right] \\ &= \frac{1}{T}\sum_{i=1}^{N}\left[p_{11}^i\Delta_i + p_{12}^i\Delta_i^2 + \frac{p_{22}^i\Delta_i^3}{3} + \frac{\sigma_\nu^2 T\Delta_i^4}{16}\right]. \end{aligned} \tag{25}$$

Similarly,

$$\mathrm{AEV_v} = \frac{1}{T}\sum_{i=1}^{N}\left[p_{22}^i\Delta_i + \tfrac{1}{2}\sigma_\nu^2 T\Delta_i^2\right] \tag{26}$$

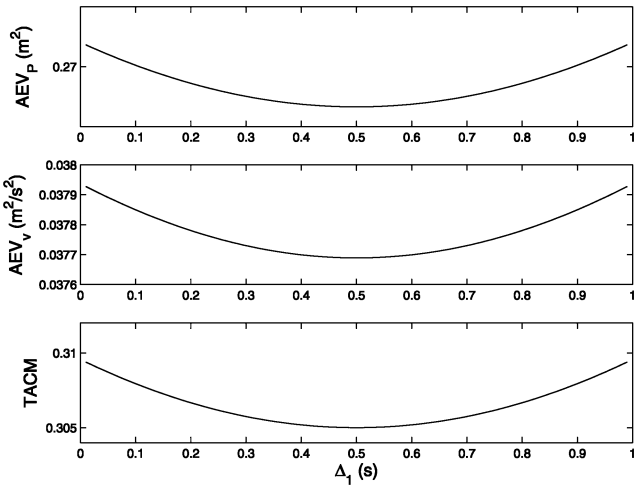

Fig. 4. Average position error variance $\mathrm{AEV_p}$, average velocity error variance $\mathrm{AEV_v}$, and trace of average covariance matrix (TACM) as functions of Δ_1. $T = 1$ s, $\sigma_\omega = 1$ m, target maneuvering index $\lambda = 0.1$.

where P^i is the steady state estimation error covariance matrix associated with the ith sensor S_i

$$P^i = \begin{bmatrix} p_{11}^i & p_{12}^i \\ p_{12}^i & p_{22}^i \end{bmatrix}. \tag{27}$$

It is very difficult to derive the closed-form of P^i when Δ_is are not identical. Instead, we compute the steady state estimation error covariance matrices numerically.

From (20), it is evident that for both the system with synchronous sensors and that with temporally staggered sensors, the trace of the average covariance matrix (TACM) is

$$\begin{aligned}\mathrm{TACM} &= \mathrm{Tr}\left[\frac{1}{T}\int_0^T P(t)dt\right] \\ &= \frac{1}{T}\int_0^T \mathrm{Tr}[P(t)]dt \\ &= \mathrm{AEV_p} + \mathrm{AEV_v}. \end{aligned} \tag{28}$$

1) *System with Two Sensors*: We now consider the simple case of a two-sensor system and present the numerically obtained results for two different values of λ. From Figs. 4 and 5, it is clear that the system attains the minimum average position and velocity error variances, and the minimum TACM, when $\Delta_1 = 0.5T$, no matter what the λ is.

This is not surprising because from (25) and (26), we know that $\mathrm{AEV_p}$ and $\mathrm{AEV_v}$ are both polynomials of staggering intervals Δ_is. The updated estimation errors (p_{ij}s) only affect the lower order terms in $\mathrm{AEV_p}$ and $\mathrm{AEV_v}$. The dominant highest order terms are independent of p_{ij}s and depend solely on Δ_is. So the best thing to do is to prevent the Δ_i from becoming too large. Due to the symmetry of the sensors, the optimal solution is staggering them uniformly over time.

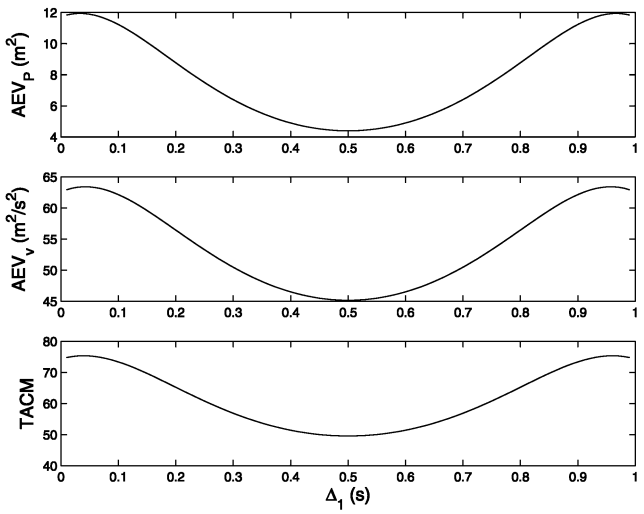

Fig. 5. Average position error variance $\mathrm{AEV_p}$, average velocity error variance $\mathrm{AEV_v}$, and trace of average covariance matrix (TACM) as functions of Δ_1. $T = 1$ s, $\sigma_\omega = 1$ m, target maneuvering index $\lambda = 10$.

Hence, even though synchronous sensors can offer better updated estimation at the update time, they do not result in smaller overall average error variance.

2) *System with Multiple Sensors*: To find the best staggering pattern for a system with N sensors is an optimization problem:

$$\min_{\vec{\Delta}} \mathrm{AEV}(\vec{\Delta}) \tag{29}$$

under the constraint that

$$\sum_{i=1}^{N} \Delta_i = T \tag{30}$$

and

$$0 \le \Delta_i \le T, \qquad i = 1,\ldots,N. \tag{31}$$

Through numerical methods, we have obtained results for the general case where a system has multiple ($N > 2$) sensors. The optimal way to attain minimum $\mathrm{AEV_p}$ and $\mathrm{AEV_v}$ is again to stagger sensors uniformly over time.

B. Performance Analysis

1) *Updated Estimation Error Variance*: A system with N uniformly staggered identical sensors is equivalent to a system with one sensor that has N times the sampling rate

$$T_1 = \frac{T}{N}. \tag{32}$$

The standard deviation (SD) of measurement noise for each sensor is

$$\sigma_{\omega_1} = \sigma_\omega. \tag{33}$$

Similar to (24), the associated process noise variance is rescaled and

$$\sigma_{\nu_1} = \sqrt{N}\sigma_\nu. \tag{34}$$

And from (9), the corresponding target maneuvering index is

$$\lambda_1 = \frac{\sigma_{\nu_1} T_1^2}{\sigma_{\omega_1}} = \frac{\sqrt{N}}{N^2}\lambda \tag{35}$$

where λ is the target maneuvering index for each individual sensor. Replacing σ_ω, T, α, β, and λ in (10), (11), and (12) with σ_{ω_1}, T_1, α_1, β_1, and λ_1 respectively, we have the steady state estimation error covariance matrix for the system with uniformly staggered sensors:

$$A = \begin{bmatrix} a_{11} & a_{12} \\ a_{12} & a_{22} \end{bmatrix} = \sigma_\omega^2 \begin{bmatrix} \alpha_1 & \dfrac{N\beta_1}{T} \\ \dfrac{N\beta_1}{T} & \dfrac{N^2\beta_1(\alpha_1 - \beta_1/2)}{T^2(1-\alpha_1)} \end{bmatrix}. \tag{36}$$

Hence the UEEV for position estimation is

$$\mathrm{UEEV_{p_1}} = \sigma_\omega^2 \alpha_1 \tag{37}$$

and the UEEV for velocity estimation is

$$\mathrm{UEEV_{v_1}} = \frac{\sigma_\omega^2}{T^2} N^2 f(\lambda_1) \tag{38}$$

where

$$f(\lambda) = \frac{\beta\left(\alpha - \dfrac{\beta}{2}\right)}{1-\alpha} = \frac{\lambda\sqrt{\lambda^2 + 8\lambda} - \lambda^2}{2}. \tag{39}$$

The performance for a centralized fusion system with N identical synchronous sensors is the same as a system with one composite sensor with variance σ_ω^2/N

$$\sigma_{\omega_2} = \frac{\sigma_\omega}{\sqrt{N}}. \tag{40}$$

For synchronous sensors, the sampling interval remains the same and there is no need to rescale the process noise variance. As a result, we have

$$T_2 = T \tag{41}$$

and

$$\sigma_{\nu_2} = \sigma_\nu. \tag{42}$$

The target maneuvering index for this composite sensor is

$$\lambda_2 = \frac{\sigma_{\nu_2} T_2^2}{\sigma_{\omega_2}} = \sqrt{N}\lambda. \tag{43}$$

Replacing σ_ω, T, α, β, and λ in (10), (11), and (12) with σ_{ω_2}, T_2, α_2, β_2, and λ_2, respectively, we have the steady state covariance matrix for the system with

synchronous sensors:

$$B = \begin{bmatrix} b_{11} & b_{12} \\ b_{12} & b_{22} \end{bmatrix} = \frac{\sigma_\omega^2}{N} \begin{bmatrix} \alpha_2 & \dfrac{\beta_2}{T} \\ \dfrac{\beta_2}{T} & \dfrac{\beta_2\left(\alpha_2 - \dfrac{\beta_2}{2}\right)}{T^2(1-\alpha_2)} \end{bmatrix}. \quad (44)$$

Therefore,

$$\mathrm{UEEV}_{\mathrm{p}_2} = \sigma_\omega^2 \frac{\alpha_2}{N} \quad (45)$$

and

$$\mathrm{UEEV}_{\mathrm{v}_2} = \frac{\sigma_\omega^2}{T^2} \frac{f(\lambda_2)}{N}. \quad (46)$$

Note that the trace of the updated covariance matrix (TUCM) is

$$\mathrm{TUCM} = \mathrm{UEEV}_{\mathrm{p}} + \mathrm{UEEV}_{\mathrm{v}}. \quad (47)$$

The relative performance of the two systems can be summarized in the following theorem.

THEOREM 1 *The system with synchronous sensors has a smaller* UEEV *and a smaller* TUCM *than that with uniformly staggered sensors, i.e.,* $\mathrm{UEEV}_{\mathrm{p}_1} > \mathrm{UEEV}_{\mathrm{p}_2}$, $\mathrm{UEEV}_{\mathrm{v}_1} > \mathrm{UEEV}_{\mathrm{v}_2}$, *and* $\mathrm{TUCM}_1 > \mathrm{TUCM}_2$.

PROOF See Appendix A.

In Figs. 6 and 7, the updated position and velocity estimation error variances for both systems are compared for $N = 2$. The system with synchronous sensors always has better performance especially when λ is high. This is just as we expected. At the update time (kT), the system with synchronous sensors updates its estimation with measurements from N sensors while the system with staggered sensors has measurements only from one sensor. Hence, the system with synchronous sensors has more information about the target and generates a more accurate estimate.

2) *Maximum Prediction Error Variance*: For a system with N uniformly staggered sensors, by replacing p_{ij} in (18) with a_{ij} in (36), we get the maximum predicted position error variance:

$$\begin{aligned} \mathrm{MPEV}_{\mathrm{p}_1} &= [a_{11} + 2a_{12}t + a_{22}t^2 + \tfrac{1}{4}\sigma_\nu^2 T t^3]|_{t=T/N} \\ &= \sigma_\omega^2 \left[\alpha_1 + 2\beta_1 + \frac{\beta_1\left(\alpha_1 - \dfrac{\beta_1}{2}\right)}{1-\alpha_1}\right] + \frac{\sigma_\nu^2 T^4}{4N^3} \\ &= \sigma_\omega^2 \left[g(\lambda_1) + \frac{\lambda^2}{4N^3}\right] \end{aligned} \quad (48)$$

where

$$\begin{aligned} g(\lambda) &= \alpha + 2\beta + \frac{\beta\left(\alpha - \dfrac{\beta}{2}\right)}{1-\alpha} \\ &= \tfrac{1}{8}\left[-\lambda^2 + 8\lambda + (\lambda+4)\sqrt{\lambda^2+8\lambda}\right]. \end{aligned} \quad (49)$$

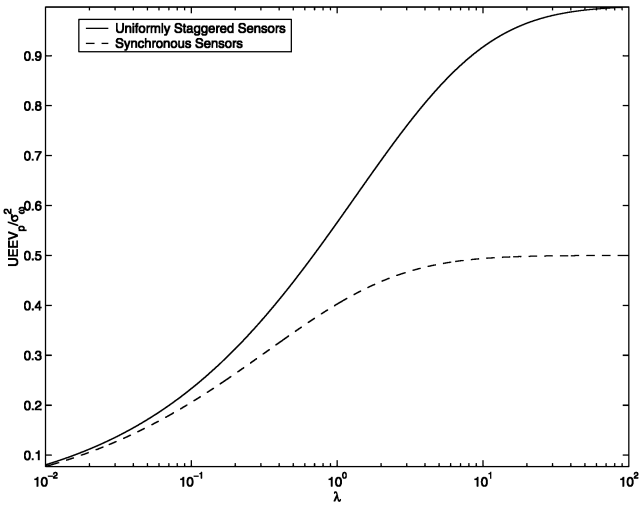

Fig. 6. Normalized updated position estimation error variance for uniformly staggered sensors and synchronous sensors ($N = 2$).

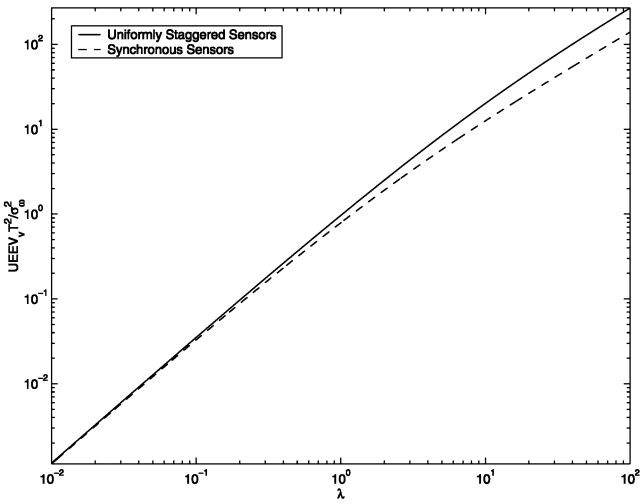

Fig. 7. Normalized updated velocity estimation error variance for uniformly staggered sensors and synchronous sensors ($N = 2$).

Replacing p_{ij} in (19) with a_{ij} in (36), the maximum predicted velocity error variance for the system with N uniformly staggered sensors is

$$\begin{aligned} \mathrm{MPEV}_{\mathrm{v}_1} &= (a_{22} + \sigma_\nu^2 T t)|_{t=T/N} \\ &= \sigma_\omega^2 \frac{N^2\beta_1\left(\alpha_1 - \dfrac{\beta_1}{2}\right)}{T^2(1-\alpha_1)} + \frac{\sigma_\nu^2 T^2}{N} \\ &= \frac{\sigma_\omega^2}{T^2}\left[N^2 f(\lambda_1) + \frac{\lambda^2}{N}\right]. \end{aligned} \quad (50)$$

For a system with N synchronous sensors, similarly, with (18) and (44) the maximum predicted position error variance is

$$\begin{aligned} \mathrm{MPEV}_{\mathrm{p}_2} &= [b_{11} + 2b_{12}t + b_{22}t^2 + \tfrac{1}{4}\sigma_\nu^2 T t^3]|_{t=T} \\ &= \sigma_\omega^2 \left[\frac{g(\lambda_2)}{N} + \frac{\lambda^2}{4}\right]. \end{aligned} \quad (51)$$

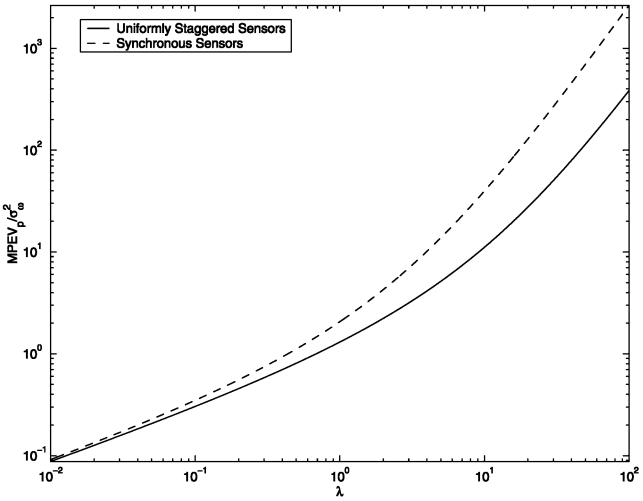

Fig. 8. Normalized maximum predicted position error variance for uniformly staggered sensors and synchronous sensors ($N = 2$).

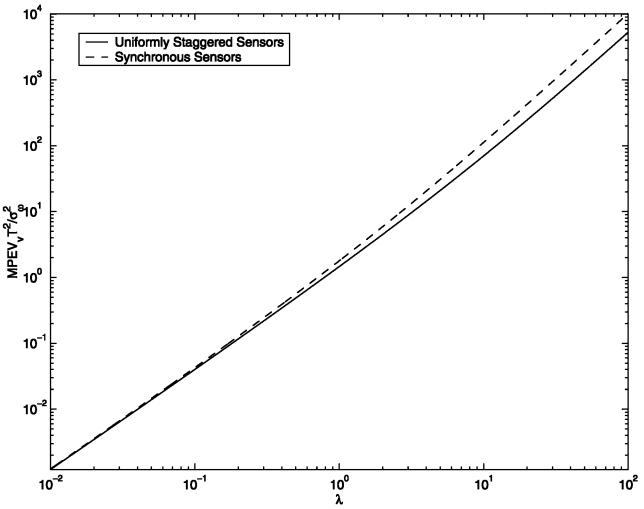

Fig. 9. Normalized maximum predicted velocity error variance for uniformly staggered sensors and synchronous sensors ($N = 2$).

With (19) and (44), the maximum predicted velocity error variance is

$$\begin{aligned}\mathrm{MPEV}_{\mathrm{v}_2} &= (b_{22} + \sigma_\nu^2 Tt)|_{t=T} \\ &= \frac{\sigma_\omega^2}{T^2}\left[\frac{f(\lambda_2)}{N} + \lambda^2\right]. \end{aligned} \tag{52}$$

The trace of the maximum covariance matrix (TMCM) is given by

$$\mathrm{TMCM} = \mathrm{MPEV}_{\mathrm{p}} + \mathrm{MPEV}_{\mathrm{v}}. \tag{53}$$

The relative performance of the two systems is given by the following theorem.

THEOREM 2 *The system with uniformly staggered sensors has a smaller* MPEV *and a smaller* TMCM *than that with synchronous sensors, i.e.,* $\mathrm{MPEV}_{\mathrm{p}_1} < \mathrm{MPEV}_{\mathrm{p}_2}$, $\mathrm{MPEV}_{\mathrm{v}_1} < \mathrm{MPEV}_{\mathrm{v}_2}$, *and* $\mathrm{TMCM}_1 < \mathrm{TMCM}_2$.

PROOF See Appendix B.

In Figs. 8 and 9, the maximum predicted position and velocity estimation error variances for systems with synchronous and uniformly staggered sensors are compared for $N = 2$. The system with uniformly staggered sensors always has better performance especially when λ is high. This is not surprising. In the system with staggered sensors, more frequent estimation updating with measurements from single sensors helps keep the maximum prediction error under control. We also observe that when target is highly maneuvering, it is more important to use staggered sensors to prevent the prediction error from getting too large.

3) *Average Error Variance*: For the system with N uniformly staggered sensors, replacing p_{ij}^i and Δ_i in (25) with a_{ij} in (36) and T/N, respectively, it is easy to get

$$\begin{aligned}\mathrm{AEV}_{\mathrm{p}_1} &= \sigma_\omega^2\left[\alpha_1 + \beta_1 + \frac{\beta_1\left(\alpha_1 - \frac{\beta_1}{2}\right)}{3(1-\alpha_1)}\right] + \frac{\sigma_\nu^2 T^4}{16N^3} \\ &= \sigma_\omega^2\left[h(\lambda_1) + \frac{\lambda^2}{16N^3}\right] \end{aligned} \tag{54}$$

where

$$\begin{aligned} h(\lambda) &= \alpha + \beta + \frac{\beta\left(\alpha - \frac{\beta}{2}\right)}{3(1-\alpha)} \\ &= \frac{(\lambda+12)\sqrt{\lambda^2+8\lambda} - \lambda^2}{24}. \end{aligned} \tag{55}$$

Replacing p_{ij}^i and Δ_i in (26) with a_{ij} and T/N, respectively, we have the average velocity error variance for a system with uniformly staggered sensors:

$$\begin{aligned}\mathrm{AEV}_{\mathrm{v}_1} &= \frac{\sigma_\omega^2}{T^2}\left[N^2\frac{\beta_1\left(\alpha_1 - \frac{\beta_1}{2}\right)}{1-\alpha_1}\right] + \frac{\sigma_\nu^2 T^2}{2N} \\ &= \frac{\sigma_\omega^2}{T^2}\left[N^2 f(\lambda_1) + \frac{\lambda^2}{2N}\right]. \end{aligned} \tag{56}$$

For the system with N synchronous sensors, replacing p_{ij} in (21) with b_{ij}, it is easy to get

$$\begin{aligned}\mathrm{AEV}_{\mathrm{p}_2} &= \frac{\sigma_\omega^2}{N}\left[\alpha_2 + \beta_2 + \frac{\beta_2\left(\alpha_2 - \frac{\beta_2}{2}\right)}{3(1-\alpha_2)}\right] + \frac{\sigma_\nu^2 T^4}{16} \\ &= \sigma_\omega^2\left[\frac{h(\lambda_2)}{N} + \frac{\lambda^2}{16}\right]. \end{aligned} \tag{57}$$

Replacing p_{ij} in (22) with b_{ij}, we have the average velocity error variance for a system with N

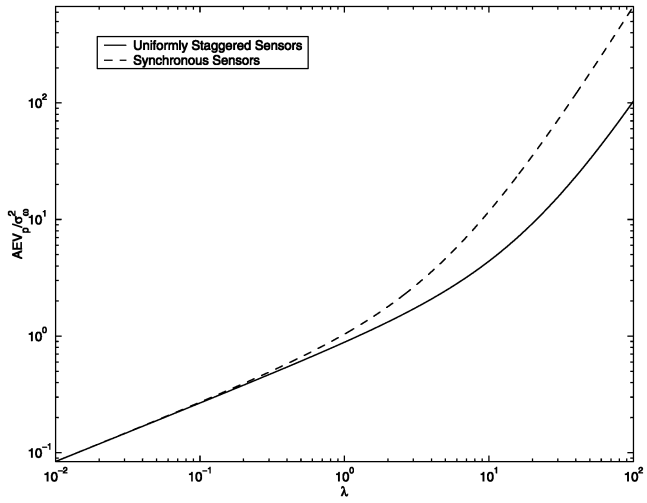

Fig. 10. Normalized average position error variance for uniformly staggered sensors and synchronous sensors ($N = 2$).

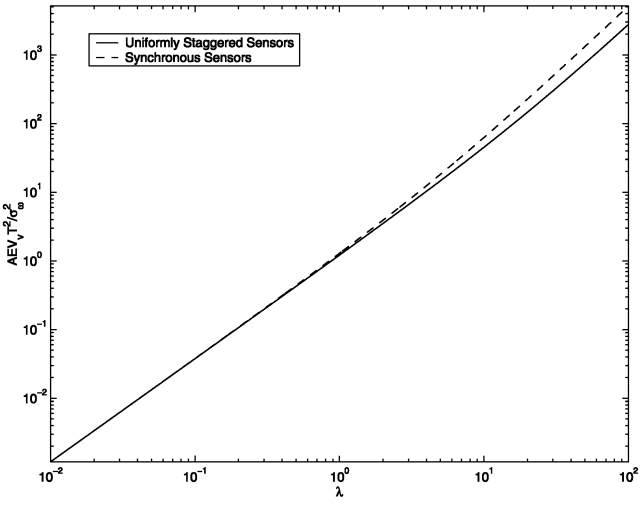

Fig. 11. Normalized average velocity error variance for uniformly staggered sensors and synchronous sensors ($N = 2$).

synchronous sensors

$$\begin{aligned}\mathrm{AEV}_{\mathrm{v}_2} &= \frac{\sigma_\omega^2}{T^2}\frac{\beta_2\left(\alpha_2-\frac{\beta_2}{2}\right)}{N(1-\alpha_2)}+\frac{1}{2}\sigma_\nu^2T^2\\ &= \frac{\sigma_\omega^2}{T^2}\left[\frac{1}{N}f(\lambda_2)+\frac{\lambda^2}{2}\right]. \end{aligned} \tag{58}$$

Once again, the relative performance of the two systems in terms of AEV is expressed as follows.

THEOREM 3 *The system with uniformly staggered sensors has a smaller* AEV *and a smaller* TACM *than that with synchronous sensors, i.e.,* $\mathrm{AEV}_{\mathrm{p}_1} < \mathrm{AEV}_{\mathrm{p}_2}$, $\mathrm{AEV}_{\mathrm{v}_1} < \mathrm{AEV}_{\mathrm{v}_2}$, *and* $\mathrm{TACM}_1 < \mathrm{TACM}_2$.

PROOF See Appendix C.

In Fig. 10, the average position variances for systems with synchronous and uniformly staggered sensors are compared. The system with uniformly staggered sensors always has better performance especially when λ is high. When $\lambda = 1$, the $\mathrm{AEV}_{\mathrm{p}_1}$ is 15% smaller than $\mathrm{AEV}_{\mathrm{p}_2}$. For $\lambda = 10$, the $\mathrm{AEV}_{\mathrm{p}_1}$ is 63% smaller than $\mathrm{AEV}_{\mathrm{p}_2}$. And as the number of sensors (N) increases, there will be even greater improvement by using uniformly staggered sensors.

The system with uniformly staggered sensors also outperforms the system with synchronous sensors in terms of average velocity error variance $\mathrm{AEV}_{\mathrm{v}}$. The curves for $\mathrm{AEV}_{\mathrm{v}_1}$ and $\mathrm{AEV}_{\mathrm{v}_2}$ are plotted in Fig. 11. From Figs. 10 and 11, we find that the two curves for uniformly staggered sensors and synchronous sensors are almost indistinguishable when λ is low ($\lambda < 0.1$). Hence we cannot gain much in terms of AEV by using staggered sensors when λ is small. Low λ means low target motion uncertainty and thus the prediction error for the system will not get too large even if we use synchronous sensors.

V. STAGGERING SENSORS WITH DIFFERENT MEASUREMENT NOISE VARIANCES

For simplicity, we only consider a system with two sensors with different measurement noise variance. We define r as the ratio between the measurement noise SD of the two sensors

$$r = \frac{\sigma_{\omega_2}}{\sigma_{\omega_1}}. \tag{59}$$

Without loss of generality, we assume that sensor S_1 is no worse than sensor S_2, i.e., $r \geq 1$. The equivalent measurement noise variance of the composite sensor (when two sensors are synchronous) can be found as follows:

$$\begin{aligned}\frac{1}{\sigma_{\omega_c}^2} &= \frac{1}{\sigma_{\omega_1}^2}+\frac{1}{\sigma_{\omega_2}^2}\\ &= \frac{1+r^2}{r^2}\frac{1}{\sigma_{\omega_1}^2}. \end{aligned} \tag{60}$$

To make fair comparisons for cases with different r, we keep $\sigma_{\omega_c}^2$, the measurement noise variance of the composite sensor, as a constant.

The results for optimal staggering patterns to attain minimum $\mathrm{AEV}_{\mathrm{p}}$ and $\mathrm{AEV}_{\mathrm{v}}$ are obtained numerically and are shown in Figs. 12 and 13, respectively. Here λ is the target maneuvering index for the composite sensor:

$$\lambda = \frac{\sigma_\nu T^2}{\sigma_{\omega_c}}. \tag{61}$$

First of all, Δ_1 is always greater than or equal to $T/2$. Since updated estimation based on sensor S_1 will be more accurate than that based on sensor S_2, intuitively the time Δ_1 should be no less than Δ_2.

Second, optimal Δ_1 for a system with a higher r is always greater than that for a system with a lower r. Higher r means that the degree of accuracy of sensor S_1 over sensor S_2 is larger, and thus estimation based

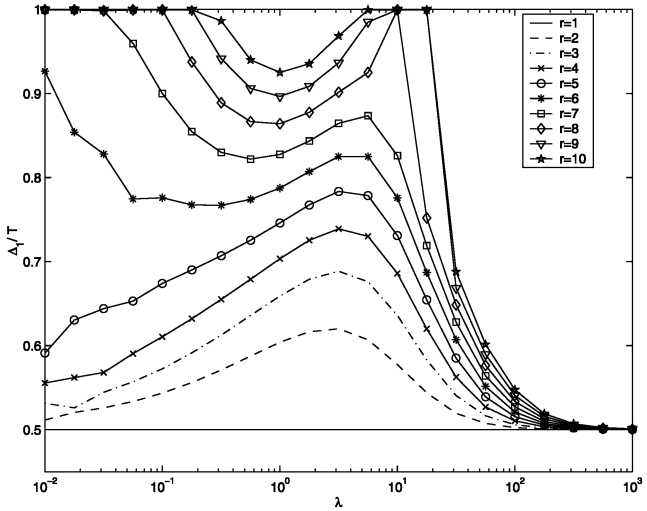

Fig. 12. Optimal staggering time Δ_1 to obtain minimum AEV_p for different measurement noise SD ratio r between the two sensors.

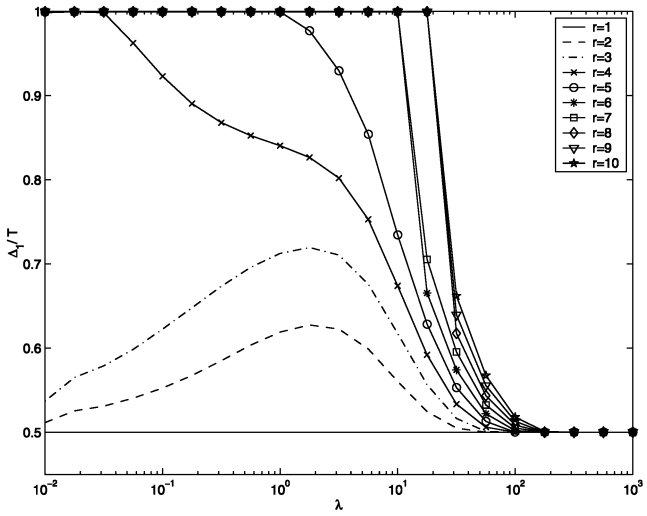

Fig. 13. Optimal staggering time Δ_1 to obtain minimum AEV_v for different measurement noise SD ratio r between the two sensors.

on sensor S_1 is used for a longer time after the system is updated with its measurement.

When λ is small, the optimal Δ_1 depends on r as follows: if r is small, meaning that measurements from the two sensors have similar quality, the Δ_1 is close to $T/2$, or the optimal pattern is close to uniform staggering; when r is large, optimal Δ_1 tends to T. This is because the accuracy of sensor S_2 is so poor compared with S_1, that the system gains little by updating with measurements from S_2 and has to be immediately updated once again with data from S_1. Hence the optimal pattern is close to using synchronous sensors. This phenomenon is evident on the left side of Figs. 12 and 13, i.e., when λ is close to 10^{-2}. For these values of λ, as r increases, Δ_1/T increases to 1.

When λ is very high, the optimal Δ_1 for both AEV_p and AEV_v tends to $T/2$ no matter what r is,

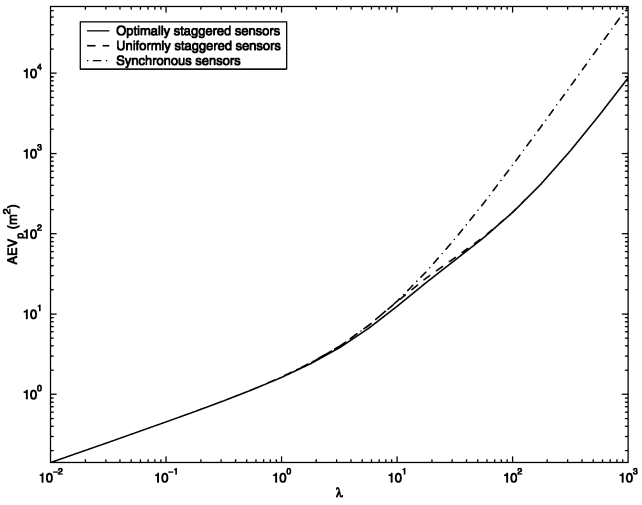

Fig. 14. Average position error variance for different staggering schemes ($r = 5$).

meaning that uniform staggering is the best pattern. This is not surprising as we have similar results for the case of equal-quality sensors. When λ (or σ_ν if σ_ω and T are fixed) is high, the last terms in (25) and (26) are dominant, and the other terms are negligible. And the effect of quality difference between S_1 and S_2 on the system are negligible. Therefore, the two sensors are symmetric in some sense under this situation.

For intermediate values of λ (λ between roughly 0.1 and 10) and relatively high values of r ($r > 4$), we observe an interesting behavior. For a given value of r in this range, as λ increases, Δ_1/T first decreases then it increases before finally decreasing to 0.5. This is due to the interplay between values of r and λ that is not obvious and not easily explained.

In Fig. 14, AEV_p for three different staggering patterns is plotted for $r = 5$. AEV_p for synchronous sensors is much worse than that of uniformly and optimally staggered sensors especially when λ is high. And the performances of uniformly staggered sensors and optimally staggered sensors are very close to each other.

To compare uniform staggering and optimal staggering schemes, we plot the ratio of their AEV_p in Fig. 15. As we can see, when r is small or medium ($r \leq 5$), the AEV_p of uniform staggering is no more than 15% worse than that of optimally staggered sensors. Even when r is as large as 10, the AEV_p for uniformly staggered sensors is still no more than 30% worse than that for optimally staggered sensors. This suggests that for simplicity, we can use uniformly staggered sensors at the cost of a little degradation in performance.

In Fig. 16, the AEV_p is plotted for the optimally staggered sensors case. In Fig. 17, the AEV_p for the optimally staggered sensors case is normalized by the AEV_p for the optimally staggered case for identical sensors ($r = 1$). Because we keep $\sigma^2_{\omega_c}$, the composite

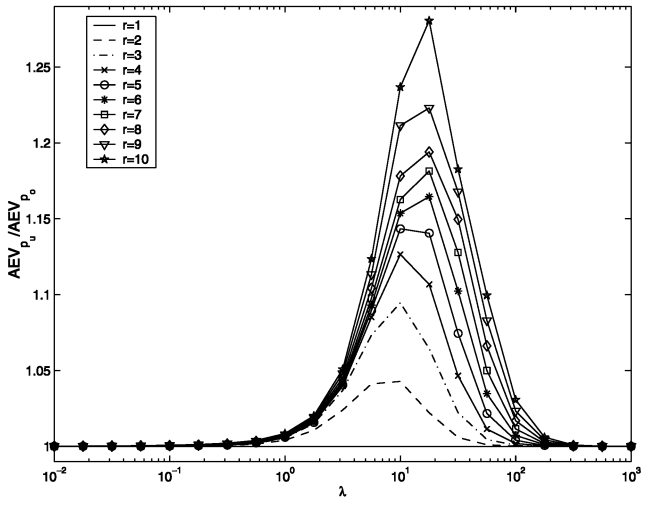

Fig. 15. Ratio between AEV_p for uniformly staggered sensors (AEV_{p_u}) and AEV_p for optimally staggered sensors (AEV_{p_o}).

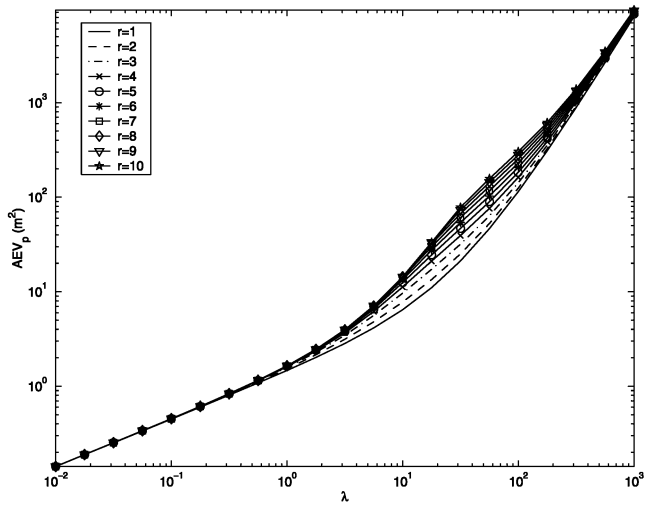

Fig. 16. AEV_p of optimally staggered sensors for different r.

sensor measurement noise variance, as a constant, we can make fair comparisons for different r. These figures show that for the same composite sensor and associated constraints, the smaller the r is, the better the performance is. This means that if we have control over how a constrained resource (the inverse of the composite sensor's measurement noise variance) is assigned to each individual sensor, we want to divide the resource evenly to two sensors and to uniformly stagger the sensors.

The results for AEV_v that we have obtained are very similar to those for AEV_p and we do not provide them here.

VI. CONCLUSIONS AND DISCUSSION

The effects of temporally staggered sensors on the target tracking performance of multi-sensor systems have been studied and a new metric-average error variance, has been defined to more accurately reflect system performance temporally.

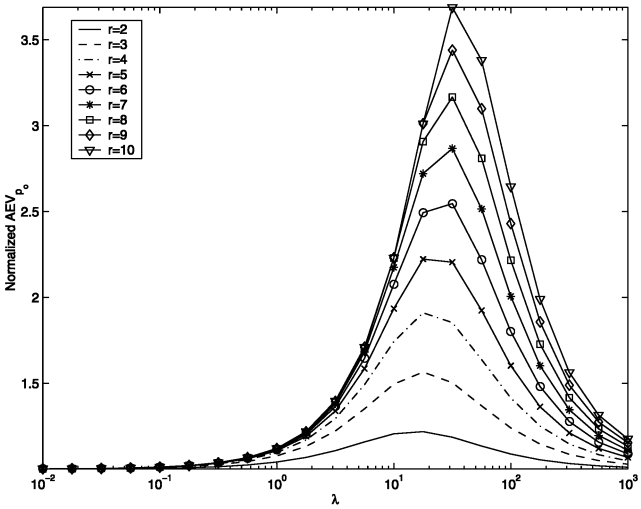

Fig. 17. AEV_p of optimally staggered sensors normalized by AEV_p of optimally staggered sensors with same measurement noise variance ($r = 1$).

For the case where sensors have the same measurement noise variances, numerical results show that it is best to use uniformly staggered sensors to obtain low AEV_p and AEV_v, especially when target maneuvering index λ is high. The higher the λ is, the more we can benefit by using temporally staggered sensors. When λ is very low or when the target motion is more predictable, there is very little improvement by using staggered sensors. Many closed-form results have been derived. We have analytically shown that the system with uniformly staggered sensors outperforms that with synchronous sensors both in terms of MPEV and AEV.

For the case where sensors have different measurement noise variance, the guideline for staggering schemes can be found via numerical methods. When the target maneuvering index λ is low or medium, we use the estimation based on the more accurate sensor for a longer time. If λ is very high, uniformly staggered sensors should be used regardless of the quality difference between measurements of different sensors. For simplicity, uniform staggering schemes can be used as an alternative with relatively small performance degradation. If we have control over system design, for a fixed resource (the inverse of the composite sensor measurement noise variance), we should always divide equal resource to each sensor and use uniform staggering schemes.

APPENDIX A. PROOF OF THEOREM 1

A. Updated Position Estimation Error Variance

According to (37) and (45), $UEEV_{p_1} > UEEV_{p_2}$ is equivalent to

$$\alpha_1 > \frac{1}{N}\alpha_2 \tag{62}$$

or

$$-\frac{1}{8}\left[\lambda_1^2+8\lambda_1-(\lambda_1+4)\sqrt{\lambda_1^2+8\lambda_1}\right] > -\frac{1}{8N}\left[\lambda_2^2+8\lambda_2-(\lambda_2+4)\sqrt{\lambda_2^2+8\lambda_2}\right]. \quad (63)$$

We define

$$\lambda_0 = \sqrt{N}\lambda. \quad (64)$$

From (35) and (43), we have

$$\lambda_1 = \frac{\lambda_0}{N^2} \quad (65)$$

and

$$\lambda_2 = \lambda_0. \quad (66)$$

Substituting these two equations into (63) and simplifying it, we have

$$\lambda_0^2+8N^2\lambda_0-(\lambda_0+4N^2)\sqrt{\lambda_0^2+8N^2\lambda_0} < N^3\left[\lambda_0^2+8\lambda_0-(\lambda_0+4)\sqrt{\lambda_0^2+8\lambda_0}\right] \quad (67)$$

or

$$N^3(\lambda_0+4)\sqrt{\lambda_0^2+8\lambda_0}-(\lambda_0+4N^2)\sqrt{\lambda_0^2+8N^2\lambda_0} < (N-1)\lambda_0[(N^2+N+1)\lambda_0+8N^2]. \quad (68)$$

We have

$$\left[N^3(\lambda_0+4)\sqrt{\lambda_0^2+8\lambda_0}\right]^2-\left[(\lambda_0+4N^2)\sqrt{\lambda_0^2+8N^2\lambda_0}\right]^2 = \lambda_0^2[(N^6-1)\lambda_0^2+16N^2(N^4-1)\lambda_0+80N^4(N^2-1)] \quad (69)$$

which is always positive as long as $N>1$ and $\lambda_0>0$. Since each term on the left side of (68) is positive, (69) proves that the left side of (68) is positive. After squaring both sides of (68) and some derivations, we get

$$\lambda_0^3+8(N^2+1)\lambda_0^2+8N(N^2+8N+1)\lambda_0+128N^3 < (\lambda_0+4)(\lambda_0+4N^2)\sqrt{\lambda_0+8}\sqrt{\lambda_0+8N^2}. \quad (70)$$

Again, after squaring both sides of the above inequality and simplifications, we get

$$(N-1)^2\lambda_0[(N^2+N+1)\lambda_0^3+8(N^4+N^3+3N^2+N+1)\lambda_0^2+4N^2(31N^2+14N+31)\lambda_0+512N^4]>0 \quad (71)$$

which always holds when $N\geq 2$ and $\lambda_0>0$.

B. Updated Velocity Estimation Error Variance

According to (38) and (46), $\mathrm{UEEV}_{\mathrm{v}_1} > \mathrm{UEEV}_{\mathrm{v}_2}$ is equivalent to

$$N^2 f(\lambda_1) > \frac{f(\lambda_2)}{N}. \quad (72)$$

Using (39) and substituting (65) and (66) into the above inequality, we have

$$\lambda_0\sqrt{\lambda_0^2+8N^2\lambda_0}-\lambda_0^2 > N\left[\lambda_0\sqrt{\lambda_0^2+8\lambda_0}-\lambda_0^2\right]. \quad (73)$$

After simplification, it becomes

$$(N-1)\lambda_0 > N\sqrt{\lambda_0^2+8\lambda_0}-\sqrt{\lambda_0^2+8N^2\lambda_0}. \quad (74)$$

Taking squares of the both sides, we have

$$\sqrt{\lambda_0+8}\sqrt{\lambda_0+8N^2} > \lambda_0+8N. \quad (75)$$

Taking squares of both sides once more, we finally have

$$(N-1)^2>0 \quad (76)$$

which is always true.

C. Trace of Updated Covariance Matrix

In Sections A and B, we have shown that $\mathrm{UEEV}_{\mathrm{p}_1} > \mathrm{UEEV}_{\mathrm{p}_2}$ and $\mathrm{UEEV}_{\mathrm{v}_1} > \mathrm{UEEV}_{\mathrm{v}_2}$. Since

$$\mathrm{TUCM} = \mathrm{UEEV}_{\mathrm{p}} + \mathrm{UEEV}_{\mathrm{v}}$$

we have

$$\mathrm{TUCM}_1 > \mathrm{TUCM}_2.$$

APPENDIX B. PROOF OF THEOREM 2

A. Maximum Predicted Position Error Variance

According to (48) and (51),

$$\mathrm{MPEV}_{\mathrm{p}_1} < \mathrm{MPEV}_{\mathrm{p}_2} \Leftrightarrow g(\lambda_1)+\frac{\lambda^2}{4N^3} < \frac{g(\lambda_2)}{N}+\frac{\lambda^2}{4}. \quad (77)$$

After substituting (64), (65), (66), and (49) into the above inequality and simplifications, we have

$$\lambda_0^2+8N^2\lambda_0+(\lambda_0+4N^2)\sqrt{\lambda_0^2+8N^2\lambda_0} < N^3\left(\lambda_0^2+8\lambda_0+(\lambda_0+4)\sqrt{\lambda_0^2+8\lambda_0}\right) \quad (78)$$

or

$$N^3(\lambda_0+4)\sqrt{\lambda_0^2+8\lambda_0}-(\lambda_0+4N^2)\sqrt{\lambda_0^2+8N^2\lambda_0} > (1-N)\lambda_0((N^2+N+1)\lambda_0+8N^2). \quad (79)$$

In addition, we have

$$\left[N^3(\lambda_0+4)\sqrt{\lambda_0^2+8\lambda_0}\right]^2-\left[(\lambda_0+4N^2)\sqrt{\lambda_0^2+8N^2\lambda_0}\right]^2 = \lambda_0^2[(N^6-1)\lambda_0^2+16N^2(N^4-1)\lambda_0+80N^4(N^2-1)] \quad (80)$$

which is positive when $N > 1$. Therefore, the left hand side of (79) is positive. The right hand side of (79) is always negative. Hence, inequality (79) holds.

B. Maximum Predicted Velocity Error Variance

According to (50) and (52), $\mathrm{MPEV}_{v_1} < \mathrm{MPEV}_{v_2}$ is equivalent to

$$N^2 f(\lambda_1) + \frac{\lambda^2}{N} < \frac{f(\lambda_2)}{N} + \lambda^2. \tag{81}$$

Using (39) and substituting (64), (65), and (66) into the above inequality, we have

$$\lambda_0 + \sqrt{\lambda_0^2 + 8N^2\lambda_0} < N\left(\lambda_0 + \sqrt{\lambda_0^2 + 8\lambda_0}\right). \tag{82}$$

Because

$$\begin{aligned} \lambda_0 &< N\lambda_0 \\ \sqrt{\lambda_0^2 + 8N^2\lambda_0} &< N\sqrt{\lambda_0^2 + 8\lambda_0} \end{aligned} \tag{83}$$

the inequality (82) always holds.

C. Trace of Maximum Covariance Matrix

In Sections A and B, we have shown that $\mathrm{MPEV}_{p_1} < \mathrm{MPEV}_{p_2}$ and $\mathrm{MPEV}_{v_1} < \mathrm{MPEV}_{v_2}$. Since

$$\mathrm{TMCM} = \mathrm{MPEV}_p + \mathrm{MPEV}_v$$

we have

$$\mathrm{TMCM}_1 < \mathrm{TMCM}_2.$$

APPENDIX C. PROOF OF THEOREM 3

A. Average Position Error Variance

From (54) and (57), we have

$$\mathrm{AEV}_{p_1} < \mathrm{AEV}_{p_2} \Leftrightarrow h(\lambda_1) + \frac{\lambda^2}{16N^3} < \frac{h(\lambda_2)}{N} + \frac{\lambda^2}{16}. \tag{84}$$

After substituting (64), (65), (66), and (55) into the above inequality and simplifications, we have

$$\begin{aligned} &\frac{\lambda_0^2(N^3-1)}{2} \\ &\quad > (\lambda_0 + 12N^2)\sqrt{\lambda_0^2 + 8N^2\lambda_0} - N^3(\lambda_0 + 12)\sqrt{\lambda_0^2 + 8\lambda_0}. \end{aligned} \tag{85}$$

First, the left side of (85) is positive. Secondly, we have

$$\begin{aligned} &\left[N^3(\lambda_0 + 12)\sqrt{\lambda_0^2 + 8\lambda_0}\right]^2 - \left[(\lambda_0 + 12N^2)\sqrt{\lambda_0^2 + 8N^2\lambda_0}\right]^2 \\ &\quad = \lambda_0^2[(N^6-1)\lambda_0^2 + 32N^2(N^4-1)\lambda_0 + 336N^4(N^2-1)] \end{aligned} \tag{86}$$

which is positive. Therefore, the right side of (85) is negative and the inequality (85) holds.

B. Average Velocity Error Variance

According to (56) and (58), $\mathrm{AEV}_{v_1} < \mathrm{AEV}_{v_2}$ is equivalent to

$$N^2 f(\lambda_1) + \frac{\lambda^2}{2N} < \frac{1}{N} f(\lambda_2) + \frac{\lambda^2}{2}. \tag{87}$$

Using (39) and substituting (64), (65), and (66) into the above inequality, we have

$$\sqrt{\lambda_0^2 + 8N^2\lambda_0} < N\sqrt{\lambda_0^2 + 8\lambda_0}. \tag{88}$$

This is always true when $N > 1$. Hence, the inequality (87) holds.

C. Trace of Average Covariance Matrix

In Sections A and B, we have shown that $\mathrm{AEV}_{p_1} < \mathrm{AEV}_{p_2}$ and $\mathrm{AEV}_{v_1} < \mathrm{AEV}_{v_2}$. Since

$$\mathrm{TACM} = \mathrm{AEV}_p + \mathrm{AEV}_v$$

we have

$$\mathrm{TACM}_1 < \mathrm{TACM}_2.$$

REFERENCES

[1] Bar-Shalom, Y., Li, X. R., and Kirubarajan, T.
Estimation with Applications to Tracking and Navigation.
New York: Wiley, 2001.

[2] Bar-Shalom, Y., and Li, X. R.
Multitarget-Multisensor Tracking: Principles and Techniques.
Storrs, CT: YBS Publishing, 1995.

[3] Bar-Shalom, Y.
Update with out-of-sequence measurements in tracking: Exact solution.
Signal and Data Processing of Small Targets: Proceedings of SPIE, Vol. 4048, Orlando, FL, Apr. 2000, 541–556.

[4] Bar-Shalom, Y., Mallick, M., Chen, H., and Washburn, R.
One-step solution
for the general out-of-sequence-measurement problem in tracking.
In *Proceedings of the 2002 IEEE Aerospace Conference*, Big Sky, MT, Mar. 2002.

[5] Chen, H., Kirubarajan, T., and Bar-Shalom, Y.
Performance limits of track-to-track fusion vs. centralized estimation: Theory and application.
In *Proceedings of the 4th International Conference on Information Fusion*, Montreal, Canada, Aug. 2001.

[6] Daum, F.
A system approach to multiple target tracking.
In Y. Bar-Shalom (Ed.), *Multitarget-Multisensor Tracking: Applications and Advances, Vol. II*, Norwood, MA: Artech House, 1992.

[7] Fitzgerald, R. J.
Simple tracking filters: Steady-state filtering and smoothing performance.
IEEE Transactions on Aerospace and Electronic Systems, **AES-16** (Nov. 1980), 860–864.

[8] Friedland, B.
Optimum steady-state position and velocity estimation using noisy sampled position data.
IEEE Transactions on Aerospace and Electronic Systems, **AES-9** (Nov. 1973), 906–911.

[9] Hall, D. L., and Llinas, J.
An introduction to multisensor data fusion.
Proceedings of the IEEE, **85**, 1 (Jan. 1997), 6–23.

[10] Mallick, M., Coraluppi, S., and Carthel, C.
Advances in asynchronous and decentralized estimation.
In *Proceedings of the 2001 IEEE Aerospace Conference, Vol. 4*, Big Sky, MT, Mar. 2001, 1873–1888.

[11] Mallick, M., Krant, J., and Bar-Shalom, Y.
Multi-sensor multi-target tracking using out-of-sequence measurements.
In *Proceedings of the Fifth International Conference on Information Fusion*, Annapolis, MD, July 2002, 135–142.

[12] Moore, J. R., and Blair, W. D.
Practical aspects of multisensor tracking.
In Y. Bar-Shalom and W. D. Blair (Eds.), *Multitarget-Multisensor Tracking: Applications and Advances, Vol. III*, Norwood, MA: Artech House, 2000.

[13] Niu, R., Varshney, P., Mehrotra, K., and Mohan, C.
Temporal fusion in multi-sensor target tracking systems.
In *Proceedings of the Fifth International Conference on Information Fusion*, Annapolis, MD, July 2002, 1030–1037.

[14] Niu, R., Varshney, P., Mehrotra, K., and Mohan, C.
Sensor staggering in multi-sensor target tracking systems.
In *Proceedings of the 2003 IEEE Radar Conference*, Huntsville, AL, May 2003.

[15] Zhang, K. S., Li, X. R., and Zhu, Y. M.
Optimal update with out-of-sequence observations for distributed filtering.
In *Proceedings of the Fifth International Conference on Information Fusion*, Annapolis, MD, July 2002, 1519–1526.

[16] Zhang, X., Willett, P., and Bar-Shalom, Y.
Aspects of measurement scheduling for tracking.
In *Proceedings of the 2002 IEEE Aerospace Conference*, Big Sky, MT, Mar. 2002.

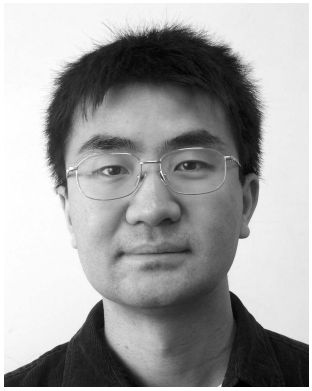

Ruixin Niu received the B.S. degree from Xi'an Jiaotong University, Xi'an, China, in 1994, the M.S. degree from the Institute of Electronics, Chinese Academy of Sciences, Beijing, in 1997, and the Ph.D. degree from the University of Connecticut, Storrs, in 2001, all in electrical engineering.

He is currently a post-doc research associate with the Syracuse University, Syracuse, New York. His research interests are in the areas of statistical signal processing and its applications, including detection, target tracking, data fusion, communications and image processing. He received the Fusion 2004 Best Paper Award, in the Seventh International Conference on Information Fusion, Stockholm, Sweden, in June 2004.

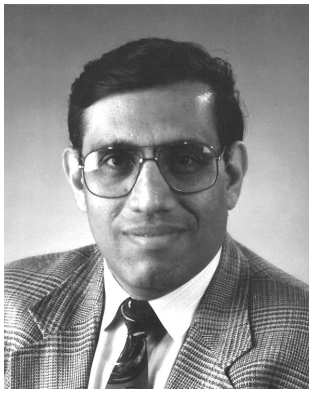

Pramod K. Varshney was born in Allahabad, India on July 1, 1952. He received the B.S. degree in electrical engineering and computer science (with highest honors), and the M.S. and Ph.D. degrees in electrical engineering from the University of Illinois at Urbana–Champaign in 1972, 1974, and 1976 respectively.

During 1972–76, he held teaching and research assistantships at the University of Illinois. Since 1976 he has been with Syracuse University, Syracuse, NY where he is currently a Professor of Electrical Engineering and Computer Science and the Research Director of the New York State Center for Advanced Technology in Computer Applications and Software Engineering. He served as the associate chair of the department during 1993–96. He is also an Adjunct Professor of Radiology at Upstate Medical University in Syracuse, NY. His current research interests are in distributed sensor networks and data fusion, detection and estimation theory, wireless communications, image processing, radar signal processing and remote sensing. He has published extensively. He is the author of *Distributed Detection and Data Fusion*, published by Springer-Verlag in 1997. He has served as a consultant to several major companies.

While at the University of Illinois, Dr. Varshney was a James Scholar, a Bronze Tablet Senior, and a Fellow. He is a member of Tau Beta Pi and is the recipient of the 1981 ASEE Dow Outstanding Young Faculty Award. He was elected to the grade of Fellow of the IEEE in 1997 for his contributions in the area of distributed detection and data fusion. He was the guest editor of the special issue on data fusion of the *Proceedings of the IEEE*, January 1997. In 2000, he received the Third Millennium Medal from the IEEE and Chancellor's Citation for exceptional academic achievement at Syracuse University. He serves as a distinguished lecturer for the AES society of the IEEE. He is on the editorial board of Information Fusion. He was the President of International Society of Information Fusion during 2001.

Kishan Mehrotra received a Ph.D. (statistics) from the University of Wisconsin at Madison, in 1971. He is currently a professor and the Computer and Information Science Program Director in the Department of Electrical Engineering and Computer Science at Syracuse University, where he has been teaching since 1970.

His research interests include pattern recognition, evolutionary algorithms, computer performance evaluation, information theory, and nonparametric statistics. He has coauthored *Elements of Artificial Neural Networks* (MIT Press, 1997), several book chapters, and over 125 journal and conference papers. He has held several offices in the American Statistical Association, and serves on the editorial board of the journal *Applied Intelligence*.

Chilukuri Mohan received a Ph.D. (computer science) from the State University of New York at Stony Brook, in 1988, and a B.Tech. (computer science) from the Indian Institute of Technology at Kanpur, in 1983.

He is currently a professor in the Department of Electrical Engineering and Computer Science at Syracuse University, where he has been teaching since 1988. He has coauthored *Elements of Artificial Neural Networks* (MIT Press, 1997), and authored *Frontiers of Expert Systems: Reasoning with Limited Knowledge* (Kluwer, 2000). He has also authored/coauthored over a hundred research papers in various areas of artificial intelligence. He is a member of an IEEE Task Force on Swarm Intelligence, and serves on several international conference committees.